ISSN 2007-9737

Segmentation of Surface Electromyography Signals: A Comparative Analysis of Time and Frequency Domain Methods

Santiago Mendez-Moreno[1,*], Laura Espinosa[2], Omar Vital-Ochoa[3], Ricardo Espinosa-Tanguma[4], Jesus Acosta-Elias[1]

[1] Universidad Autónoma de San Luis Potosí, Facultad de Ciencias, San Luis Potosí, Mexico

[2] Unidad Médica de Alta de Especialidad Dr. Victorio de la Fuente Narváez, Unidad de Medicina Física y Rehabilitación Norte, Mexico

[3] Universidad Autónoma de San Luis Potosí, Facultad de Ingeniería, San Luis Potosí, Mexico

[4] Universidad Autónoma de San Luis Potosí, Facultad de Medicina, San Luis Potosí, México

santiago.mendez.moreno@gmail.com, {jacosta, ovital, espinosr}@uaslp.mx

Abstract. This study evaluates the efficiency of computational segmentation methods in electromyographic (EMG) signal analysis across two distinct exercise sets. Twenty participants were engaged, performing a series of isometric and isotonic exercises. The first set included four isometric handgrip exercises, while the second set consisted of four isometric exercises with measured weights and two isotonic exercises with weights. Out of the total, 15 registries from the first set and 18 from the second set were considered valid. The segmentation methods assessed were RMS, Integral, Variance, Mean, and Entropy. Entropy, with a beta factor of 5, demonstrated the highest segmentation efficiency of 0.88 for the first set and 0.75 for the second. The findings highlight the potential of the Entropy method in enhancing the accuracy of EMG signal segmentation, which is crucial for the development of biomechanical models and rehabilitation protocols.

Keywords. Electromyography, signal segmentation, spectral entropy, spectral analysis.

1 Introduction

Surface electromyography (sEMG) has emerged as an invaluable instrument in biomechanics and rehabilitation, offering unique insights into muscular function that elude other methods [18, 4].

This technology, however, is often viewed through a lens of assumed efficacy, overlooking the intricate and varied challenges it presents in signal segmentation.

The prevalent application of sEMG belies the nuanced complexity inherent in interpreting muscle contractions, noise interference, and the need for precise temporal resolution.

This oversight has led to a lack of comprehensive comparative studies on segmentation methodologies. Contrary to the conventional perception of sEMG as a straightforward diagnostic tool, the segmentation of its signals is a multifaceted challenge.

Different methodologies, such as windowing techniques and overlap rates, crucially influence the accuracy and efficiency of signal processing [41, 29, 6]. Our study intends to bridge this gap by presenting a comparative analysis of computational approaches for sEMG signal segmentation. We evaluate these methods not only in terms of their efficiency but also their accuracy in various conditions.

Through this exploration, we aim to shed light on the subtleties of signal behavior and refine the techniques for dissecting these intricate biological signals. Such advancements are imperative to solidify the reliability of sEMG as both a diagnostic and interactive modality, moving beyond the realm of assumed effectiveness to a domain of proven efficacy and precision [16].

1.1 Challenges in sEMG Signal Segmentation

Surface Electromyography (sEMG) has been a pivotal tool in various fields such as medical diagnostics, sports science, and rehabilitation. The technique offers a non-invasive approach to measure muscle activation, providing valuable insights into neuromuscular functioning.

However, one of the significant challenges in sEMG data analysis is the segmentation of the recorded signals. Proper segmentation is crucial for accurate feature extraction and subsequent data interpretation. Various methods have been proposed to tackle this issue, each with its own set of advantages and limitations [21, 3, 2, 1].

Traditional methods for sEMG segmentation have been widely studied and implemented. Techniques such as Root Mean Square (RMS) have been popular for their computational efficiency [28, 12].

However, these methods often come with limitations. Moving Average and Mean Frequency are other commonly used methods, but they too require manual tuning of parameters, making them less robust for automated analysis [26]. To address these limitations, methods that doesn't rely in the amplitude of the signal, such as non-linear methods, have been proposed for sEMG segmentation.

One such promising approach is the use of Shannon Entropy, a measure of the information content in signals [5]. Unlike traditional methods, Shannon Entropy does not rely solely on the amplitude of the signal, thereby offering a more comprehensive analysis [5]. This makes it particularly useful for detecting muscle activations that may otherwise be overlooked by amplitude-based methods [13]. The standard procedure for determining the threshold for these methods often involves calculating the mean and standard deviation of the baseline noise in the sEMG signal [39]. Typically, the threshold is set as the mean plus two standard deviations.

However, this approach may not be robust enough to capture all the relevant activities in the signal, especially those with low amplitude [8]. Shannon Entropy, being a nonlinear method, offers an alternative that does not rely solely on the amplitude of the signal, potentially capturing more nuanced activities [19]. In this study, we aim to compare the efficacy of Shannon Entropy with other commonly used methods for sEMG segmentation, such as Root Mean Square (RMS), Moving Average, Mean Frequency, Skewness, Kurtosis, and Integration [28].

Each of these methods has its own set of advantages and limitations.Root Mean Square (RMS) is commonly employed in EMG analysis due to its effectiveness in steady-state conditions, yet it may not fully capture the dynamic changes inherent in non-stationary signal behaviors as seen in [28]. On the other hand, methods like Mean Frequency can be computationally expensive and may not be suitable for real-time applications [14]. Therefore, a comprehensive comparison is essential to identify the most effective and efficient method for sEMG segmentation.

2 Background

In surface electromyography (sEMG), segmentation techniques are crucial for isolating specific muscle activities or exercises from continuous recordings. One of the most common approaches is threshold-based segmentation, which is often cited for its simplicity and computational efficiency.

A study by Phinyomark et al. [28] specifically addresses the use of threshold-based methods in sEMG, highlighting its effectiveness in various applications. Despite the widespread acknowledgment of threshold-based methods in practice, it is somewhat surprising to find a limited number of research papers that focus solely on this technique within the sEMG context.

This discrepancy between practical usage and academic documentation could be attributed to several factors. One possibility is that the method is so fundamental that it is often included as a component in broader studies rather than being the focus of the research itself.

Another explanation could be that researchers in the sEMG field are more inclined to explore novel or complex methods, thereby sidelining the more straightforward threshold-based techniques.

Given this gap in the literature, it becomes pertinent to consider methodologies from other domains that also employ threshold-based segmentation techniques. For instance, a study by [7] discusses a fast video segmentation algorithm that employs shadow cancellation, global motion compensation, and adaptive threshold techniques.

Although the context is different, the underlying principles of threshold-based segmentation remain consistent and could potentially be adapted for sEMG applications.

Similarly, another study by [31] explores the use of seed growth and threshold techniques for skull stripping and automatic segmentation of brain MRI. While the application is far removed from sEMG, the segmentation techniques employed could offer valuable insights for similar challenges in sEMG data processing.

The lack of extensive research specifically tailored to sEMG segmentation necessitates a broader look into other fields where threshold-based techniques have proven effective. This interdisciplinary approach could pave the way for innovative methodologies in sEMG segmentation, filling the existing research gap.

3 Methodology

3.1 Registry Obtention

3.1.1 Participant Demographics

The study involved a cohort of 20 individuals, comprising 8 women and 12 men aged between 18 and 25. The average Body Mass Index (BMI) of the participants was 23.29, falling within the normal range. Out of these, 15 registries from the first set of exercises and 18 from the second set were deemed valid for analysis.

3.1.2 Experimental Setup

Each participant was subjected to two series of exercises. The first series included four isometric maximum strength exercises, and the second series comprised four isometric measured weight exercises and two isotonic measured weight exercises. Data was collected using a superficial electromyography (sEMG) system (MP36R Biopac), sampled at a rate of 2 kHz using Biopac software.

3.1.3 Data Collection Procedure

For the first set, participants were seated on a school chair, blindfolded, with their dominant arm supine on the school chair's palette. Electrodes were strategically placed and restraints were applied at the carpal and antebrachial heights. For the second set, electrodes were strategically placed, participants stood up, blindfolded, with their dominant arm flexed at a 90° elbow angle.

3.1.4 Exercise Protocol

For the first series, the subjects were instructed to exert maximum force by closing their hand around a ball four times for 2 seconds with 2 second interval between excertions. For the second series, the exercises involved holding weights of 2, 4, and 8 Kg exceting isometric force, followed by two isotonic exercises with 2 and 4 Kg weights. Each recording session commenced 2 seconds before the force exertion and included a minimum of 2-second intervals between exercises.

Upon completion, participants were given candy to replenish glucose levels.

3.1.5 Data Integrity and Recording

Registries were selectively excluded due to anomalies or deviations from the prescribed exercise protocol. These deviations included channel saturation, extended duration of exercises beyond the specified time, or the absence of designated resting periods between exercises.

3.2 Signal Processing

The raw sEMG signals undergo two primary types of analyses: time-domain and frequency-domain.

3.2.1 Time-Domain Analysis

Root Mean Square (RMS). The Root Mean Square (RMS) is a measure of the magnitude of a varying quantity. It is commonly used in sEMG analysis to quantify muscle activity [15, 28]. The RMS is mathematically defined as:

$$\mathrm{RMS} = \sqrt{\frac{1}{N}\sum_{n=0}^{N-1} x[n]^2}, \tag{1}$$

where N is the number of samples and $x[n]$ is the n^{th} sample. The RMS is particularly useful for capturing the power content of the signal [8, 39].

Moving Average (MAV). The Moving Average (MAV) is not used in this study due to its inherent limitations. While MAV is a simple method for smoothing signals, it is highly dependent on the amplitude of the signal. When applied directly to the raw sEMG signal, the result is essentially polar in nature, making it unsuitable for threshold-based segmentation.

Furthermore, MAV often requires the output of another process, such as the integral of the signal, to be meaningful. Due to these limitations, MAV does not provide additional information useful for sEMG segmentation.

$$\mathrm{MAV}_t = \frac{1}{n}\sum_{i=t-n+1}^{t} x_i. \tag{2}$$

Integral. The Integral of the signal is used to find the area under the curve of the sEMG signal within a specific time window. It is defined in the discrete form as:

$$\text{Integral} = \sum_{i=a}^{b} x[i], \tag{3}$$

where a and b define the sample range within the time window. The integral method is commonly used in various fields of mathematical analysis and has been applied in different contexts, such as solving non-linear differential equations [38] and fluid flow models [37].

In the context of sEMG, the integral method can be useful for motion estimation [36]. However, it is worth noting that the integral method alone may not be sufficient for sEMG segmentation and often requires additional processing or feature extraction methods to be effective.

3.2.2 Frequency-Domain Analysis

Short-Time Fourier Transform (STFT). The Short-Time Fourier Transform (STFT) is employed to analyze the frequency content of the sEMG signals within small time intervals. This provides a time-frequency representation of the signal, allowing for a more detailed analysis. The STFT is mathematically defined as:

$$\mathrm{STFT}(x(t)) = \sum_{n=-\infty}^{\infty} x(n)w(n-m)e^{-j\omega n}, \tag{4}$$

where $w(n)$ is the window function, m is the time index, and ω is the angular frequency. The STFT has been widely used in sEMG analysis for various applications such as muscle fatigue assessment and gait analysis [33, 17, 10].

Variance. In the frequency-domain analysis of sEMG signals, Variance is another commonly used feature. Variance measures the dispersion of the signal amplitude from its mean value. Mathematically, the variance σ^2 of a discrete signal $x[n]$ with N samples is given by:

$$\sigma^2 = \frac{1}{N}\sum_{n=1}^{N}(x[n]-\mu)^2, \tag{5}$$

First Set										
	RMS		Integral		Variance		Mean		Entropy	
	TS	RS	TS	RS	TS	RS	TS	RS	TS	RS
1	4	4	4	4	5	4	4	4	4	4
2	0	0	0	0	27	3	4	4	4	4
3	2	0	2	0	4	4	3	3	3	2
4	18	2	1	0	0	0	1	0	5	4
5	3	2	4	4	7	3	4	4	4	4
6	4	4	4	4	6	3	4	4	4	4
7	4	4	4	4	21	3	4	4	4	4
8	4	4	11	3	0	0	10	3	8	3
9	4	4	4	4	8	3	4	4	4	4
10	1	0	1	0	0	0	4	4	5	4
11	2	0	4	4	6	3	3	2	2	1
12	4	4	4	4	17	3	4	4	4	4
13	5	3	7	3	0	0	8	3	11	3
14	5	3	5	4	4	4	5	3	5	4
15	0	0	0	0	0	0	7	3	6	4

Second Set										
	RMS		Integral		Variance		Mean		Entropy	
	TS	RS	TS	RS	TS	RS	TS	RS	TS	RS
1	5	4	5	4	2	0	7	6	7	6
2	7	3	5	4	1	0	6	6	7	6
3	9	3	5	4	1	0	7	6	7	6
4	6	6	5	4	4	2	6	6	6	6
5	5	4	5	4	0	0	5	4	7	6
6	5	4	5	4	3	0	5	4	5	4
7	6	6	5	4	3	0	6	6	5	4
8	5	4	5	4	0	0	5	4	5	4
9	6	6	6	6	1	0	6	6	6	6
10	5	4	5	4	0	0	5	4	5	4
11	3	0	3	0	0	0	3	0	3	0
12	4	2	4	2	0	0	4	2	4	2
13	5	4	4	2	1	0	5	4	6	6
14	4	2	4	2	1	0	5	4	5	4
15	5	4	4	2	1	0	5	4	6	6
16	5	4	4	2	1	0	5	4	5	4
17	5	4	5	4	0	0	5	4	5	4
18	5	4	5	4	0	0	5	4	5	4

Fig. 1. On the left, the raw results for the first set of excercises (4 total expected). On the right, for the second set (6 total expected)

where μ is the mean of the signal. Variance is particularly useful in capturing the signal's amplitude fluctuations. However, it's worth noting that variance alone may not provide a comprehensive understanding of the muscle's condition and is often used in conjunction with other time and frequency domain features for a more robust analysis [13, 33].

Mean. The Mean is another feature commonly used in the frequency-domain analysis of sEMG signals. Mathematically, it is calculated as:

$$\text{Mean} = \frac{1}{N}\sum_{i=1}^{N} x_i, \tag{6}$$

where N is the number of frequency components and x_i is the i^{th} frequency component. The Mean is often used in conjunction with other features to provide a comprehensive understanding of the signal characteristics. For instance, [11] utilized the Mean along with time-domain features like root mean square ratio and autoregressive model for gesture recognition using sEMG signals.

[34] also incorporated the Mean in a feature set that included both time and frequency domain features for motion intention detection . [13] used the Mean as part of a multiple feature combination approach, which also included time-domain, wavelet, and fuzzy entropy features, for human gait recognition.

Skewness and Kurtosis. Skewness and kurtosis are statistical measures often used to describe the distribution of a dataset. However, these measures are not utilized in this study for the segmentation of sEMG signals. One reason could be that skewness and kurtosis can yield polar or chaotic results that may not be conducive to effective segmentation. While skewness measures the asymmetry of the data distribution, and kurtosis quantifies the "tailedness" of the distribution, their applicability in sEMG segmentation remains questionable. Therefore, this study omits these measures to focus on more reliable metrics for sEMG signal segmentation:

$$\text{Skewness} = \frac{n}{(n-1)(n-2)}\sum_{i=1}^{n}\left(\frac{x_i-\bar{x}}{s}\right)^3, \tag{7}$$

$$\text{Kurtosis} = \frac{n(n+1)}{(n-1)(n-2)(n-3)}, \tag{8}$$

$$\sum_{i=1}^{n}\left(\frac{x_i-\bar{x}}{s}\right)^4 - \frac{3(n-1)^2}{(n-2)(n-3)}, \tag{9}$$

where:

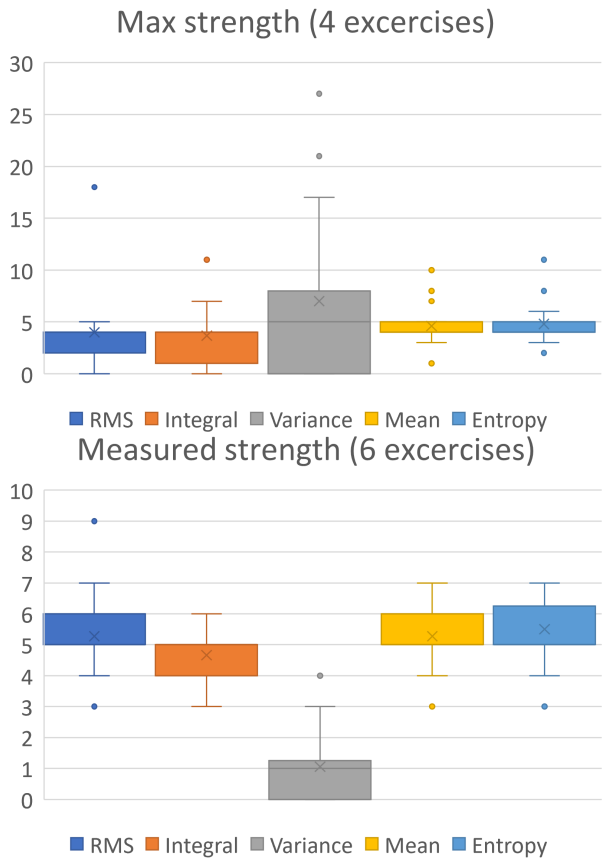

Fig. 2. On the left, the mean and dispersion for every method in the first set of exercises (4 total expected), where mean and entropy showed the least dispersion and more accuracy in segmentation. On the right, for the second set (6 total expected), with similar results for mean and entropy

n = Number of observations in the dataset.
x_i = Each individual observation in the dataset.
$\bar{x}$ = The sample mean, calculated as $\frac{1}{n}\sum_{i=1}^{n} x_i$.
s = The sample standard deviation, which is the square root of the sample variance.

Mean Frequency. Mean Frequency is excluded from this study as it provides results that are too constant to be useful for segmentation purposes. The method's output does not vary significantly across different muscle activities, making it unsuitable for isolating specific muscle activities in the continuous sEMG recordings:

$$\mathrm{MF} = \frac{\sum_{f=1}^{N} f \cdot P(f)}{\sum_{f=1}^{N} P(f)}, \tag{10}$$

where:
f = Frequency component within the signal.
$P(f)$ = Power spectral density of the frequency component f.
N = Total number of discrete frequency components in the signal.

Shannon's Entropy. Shannon's Entropy is used to measure the information content in the signal. It is particularly useful for the segmentation of sEMG signals due to its ability to capture the complexity and randomness in the data. The mathematical definition is given by:

$$H(X) = -\sum_{i=1}^{n} p(x_i) \log_n p(x_i), \tag{11}$$

where $p(x_i)$ is the probability mass function of the signal. This method is based on the foundational work on information theory by [30].

3.3 Threshold Segmentation Algorithm

The algorithm reads the first 500 samples, presumed to be basal noise, to calculate the mean (μ). This mean is then multiplied by a β factor to determine the threshold (T):

$$T = \mu \times \beta. \tag{12}$$

The β factor is found through iteration, the factor that yields better results is the one selected for every method.

3.4 Comparative Analysis

The final step involves comparing the segmentation results from each method to evaluate their efficacy and efficiency in isolating specific muscle activities from the continuous sEMG recordings.

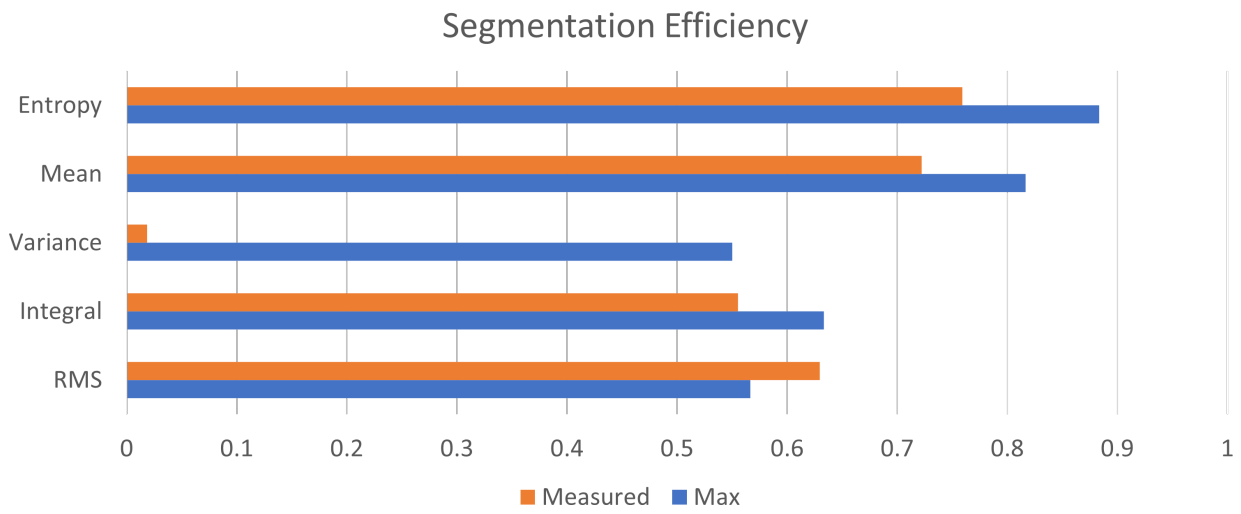

Fig. 3. Efficiency comparison of sEMG signal segmentation methods. The bar graph illustrates the segmentation efficiency for various computational methods, including Entropy, Mean, Variance, Integral, and RMS, comparing measured efficiency values against their respective maximum potentials. Entropy demonstrated the highest efficiency (0.88), confirming its robustness across different exercise sets, while Variance had the lowest performance, indicating inconsistencies in diverse exercise scenarios. The findings support the effectiveness of non-linear methods, particularly Entropy, in enhancing EMG signal segmentation accuracy

4 Results

The initial analysis of the segmentation results is illustrated in Figures 1 and 2, which present tables summarizing the outcomes of the computational techniques applied to sEMG datasets. "TS" represents 'Total Segments', indicating the segments that were longer than one second—this duration is considered the minimum expected for an exercise. "RS" denotes 'Real Segments', referring to the segments that accurately match the expected results.

To quantify these, each segment was visually evaluated against the sEMG activity; a segment was classified as 'real' if it aligned with the observable sEMG activity. Subsequently, the aggregate data were subjected to statistical analysis to calculate the average number of segments produced by each technique, as well as the deviation of the total results from the expected outcomes, in terms of mean and standard deviation. Finally, the obtained results were compared to the total expected segments (the total exercises recorded), thus determining the efficiency of each method employed.

4.1 Comparative Analysis of Segmentation Methods

Root Mean Square (RMS). The RMS method demonstrated a moderate level of segmentation success across both exercise sets with $\beta = 3$. In the first set, it achieved an average of 4 successful segmentations with a higher variability indicated by a standard deviation of 4.07.

The second set saw an improvement in both the mean number of successful segmentations, at 5.28, and a reduced standard deviation of 1.21. This suggests that the RMS method may be more suited to the conditions presented in the second set of exercises.

Integral. The Integral method showed a consistent performance with a mean of 3.67 successful segmentations in the first set and a slight improvement to 4.67 in the second set with $\beta = 4$. The low standard deviations of 2.72 and 0.65, respectively, indicate a reliable performance across different exercise protocols. This method's stability is evident in the results, as seen in Figure 2.

ISSN 2007-9737

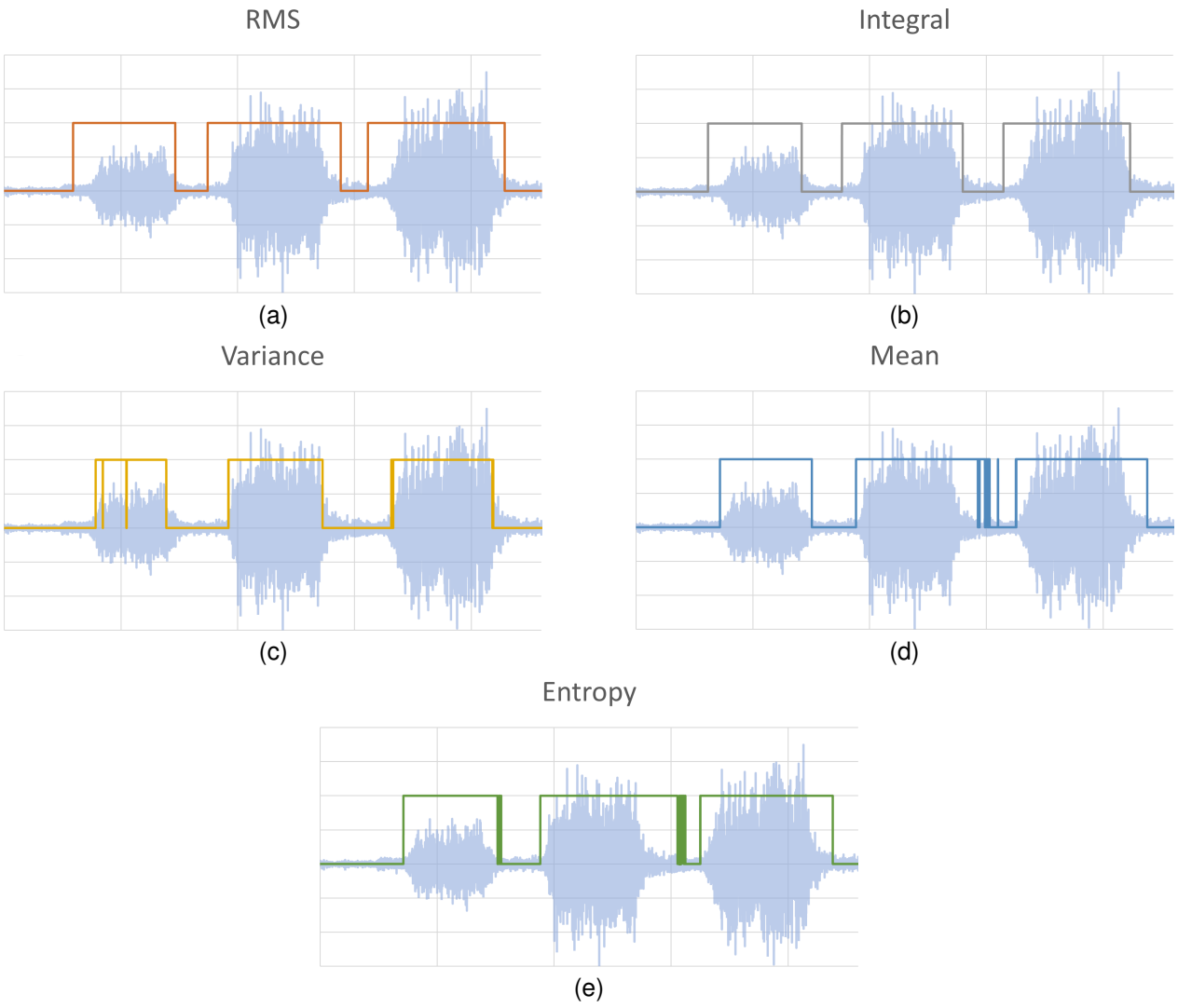

Fig. 4. Visual comparison of sEMG signal segments obtained using different methods. In (a) the segments obtained for a random registry with RMS; in (b), with Integral; in (c), Variance;(d), Mean; and (e), Entropy. Thoug the registry is random, the results shown are all for the same registry. Not all the registry is shown for practical purposes and axis informations is ignored due to the subjectivity of the comparison

Variance. Variance had the most significant discrepancy between the two sets with $\beta = 10000$. It recorded a high mean of 7 successful segmentations in the first set but a substantial standard deviation of 8.02, suggesting inconsistent results. Conversely, the second set showed a mean of only 1.06 with a slightly improved standard deviation of 1.15, indicating a general lack of reliability for this method across both sets.

Mean. The Mean method's performance was consistent with an average of 4.6 successful segmentations in the first set and a comparable mean of 5.28 in the second set with $\beta = 7$. The standard deviations of 2.12 and 0.91, respectively, reflect a stable performance with slightly better consistency in the second set. The Mean method's reliable detection across both sets is depicted in Figure 2.

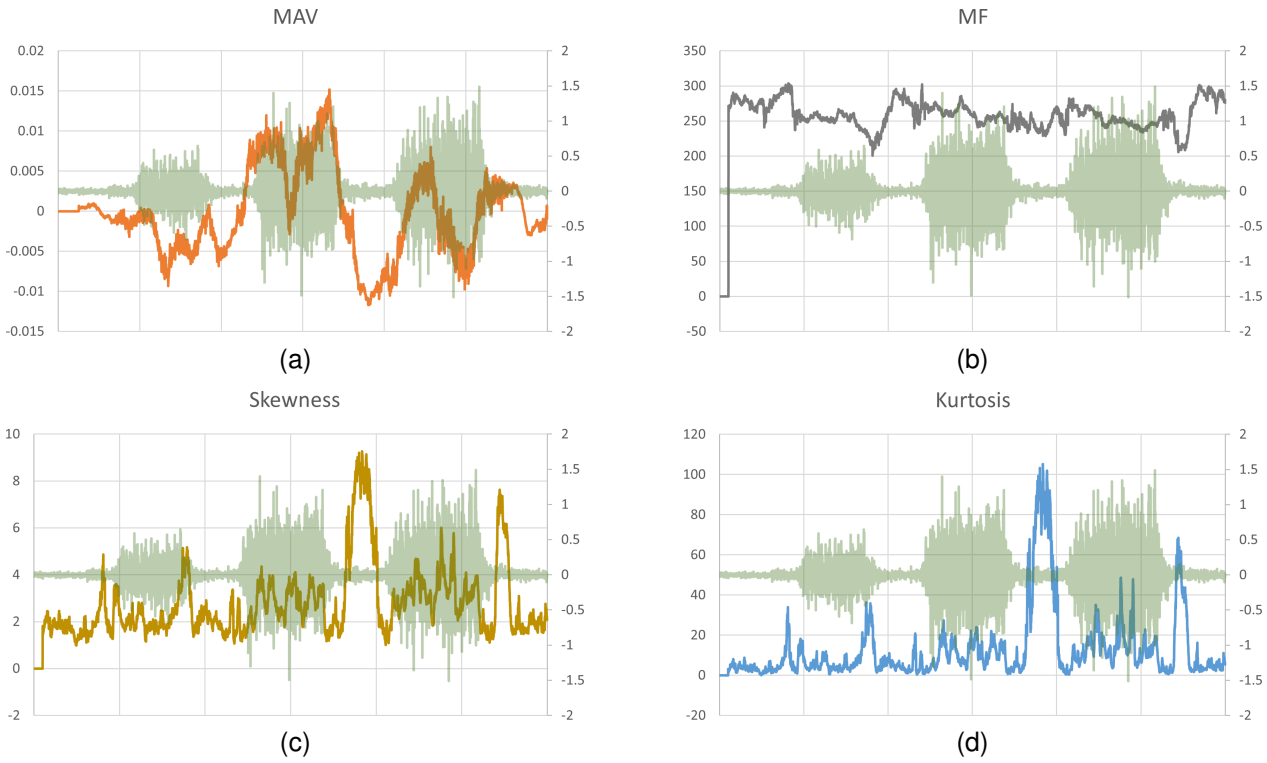

Fig. 5. Comparative results previous to segmenting using various methods on sEMG signals. Graph (a) illustrates the Moving Average method, which shows excessive smoothing of the signal, obscuring vital transient information. Graph (b) depicts the Mean Frequency method, lacking clear segmentation cues due to uniform frequency content. Graph (c) demonstrates the Skewness method, resulting in erratic segmentation not aligned with physiological events. Graph (d) presents the Kurtosis method, which overemphasizes outliers, failing to capture the overall muscle activity pattern. These methods were ultimately not selected for the final analysis due to their limitations in accurately delineating muscle contractions

Entropy. Entropy stood out as the most efficient method in both sets with $\beta = 5$. It not only had the highest mean of successful segmentations at 4.8 and 5.5 for the first and second sets, respectively, but also maintained a low standard deviation, especially in the second set with a value of 1.04. This method's superior performance and consistency highlight its potential as a robust tool for EMG signal segmentation, as illustrated in Figure 2.

4.2 Efficiency of Segmentation Methods

The efficiency of each segmentation method was further analyzed through a clustered bar graph, as depicted in Figure 3.

This graph illustrates the proportion of successful segmentations compared to the total expected segments for each method, encompassing both sets of exercises.

The efficiency of every method is scaled from 0 to 1, where 1 represents 100% accuracy in detection. However, this does not necessarily mean that only the expected segments were identified; instead, it indicates that all segments of interest were detected as anticipated.

Root Mean Square (RMS). For the RMS method, the first set of exercises showed an efficiency rate of 0.567, which slightly improved in the second set to 0.630.

This incremental increase suggests a better adaptation of the RMS method to the varied conditions of the second exercise set.

Integral. The Integral method's efficiency decreased from the first to the second set, moving from 0.633 to 0.556. This suggests that while the Integral method was relatively efficient in the first set, it did not adapt as well to the conditions of the second set of exercises.

Variance. The Variance method showed a significant drop in efficiency, from 0.550 in the first set to a mere 0.019 in the second set. This drastic decrease indicates that the Variance method may not be suitable for the type of exercises included in the second set.

Mean. The Mean method exhibited a high efficiency in the first set at 0.817, which decreased to 0.722 in the second set. Despite the drop, the Mean method still maintained a relatively high efficiency across both sets.

Entropy. Entropy proved to be the most efficient method in the first set with an efficiency rate of 0.883. It experienced a slight decrease in the second set to 0.759, yet it remained the most efficient method overall. The consistent performance of the Entropy method underscores its robustness in segmenting EMG signals across different exercise protocols.

These results, depicted in the clustered bar graph of Figure 3, highlight the varying levels of efficiency across different segmentation methods and exercise sets. The Entropy method consistently outperformed the others, affirming its potential as a reliable tool for EMG signal analysis.

5 Discussion

5.1 Electrode Placement on Biceps Brachii and Long Hand Flexor

Electrode placement for electromyographic (EMG) studies is a crucial step in ensuring the accuracy of muscle activity recordings. For the biceps brachii and the long hand flexor, electrodes are strategically positioned away from the neuromuscular junction (NMJ) to mitigate the complex interference patterns that can obscure signal interpretation.

Particularly for the biceps brachii, the NMJ is located near the center of the muscle belly; hence, electrodes are placed along the muscle fibers to more effectively capture the propagation of action potentials, avoiding the dense motor endplates that generate interference [23].

Likewise, for the long hand flexor—a deeper muscle with a more intricate structure—the challenge and discomfort of NMJ placement, along with the risk of signal attenuation, necessitate a strategic electrode positioning. This approach ensures a clear recording of muscle activity, devoid of the interference that NMJ placement might introduce [20, 9].

The judicious placement of electrodes not only enhances comfort for participants but also yields a standardized data collection process that enhances the comparability of EMG data across various studies and sessions [27].

Significantly, it reduces the incidence of movement artifacts, a vital consideration during the dynamic exercises that engage the biceps brachii and long hand flexor, thereby ensuring that the sEMG signal segmentation methods evaluated in this study are based on the most accurate and artifact-free data possible [24].

5.2 Segment Quality

The segmentation of sEMG signals is pivotal for accurate analysis, yet it is fraught with challenges due to the inherent variability in muscle contraction initiation and the presence of crosstalk. The onset of muscle contraction, marked by membrane polarization, is not always captured at the beginning of the sEMG segments.

Ideally, segments should begin with the onset of muscle polarization rather than during the summation of waves. In this context, entropy-based segmentation appears to provide segments of higher 'quality,' initiating prior to the apparent wave summation and concluding post the evident cessation of sEMG activity [25].

The operative term 'evident' is subjective, given the current lack of a definitive method to pinpoint the exact moment of membrane polarization across the motor units within a muscle, particularly when considering the impact of crosstalk.

A visual inspection of segmented sEMG signals, as depicted in Figure 4, suggests that entropy and RMS-based methods may offer superior segmentation quality. However, this observation is specific to the data set and may not generalize.

Despite the suboptimal segment quality across different methods, a segment is considered successful if it captures the essence of the sEMG activity relevant to the study's objectives, which may not necessarily include the ascending and descending tails of the signal, especially in event characterization [25].

If segment quality were a more significant factor, the efficiency rates for each method would vary considerably, with only entropy and mean potentially remaining as acceptable segmentation approaches. This is supported by the findings of Makaram and Ramakrishnan, who demonstrated the efficacy of multiscale features in distinguishing sEMG signals under various conditions, which could be particularly relevant when considering segment quality in relation to muscle fatigue [25].

5.3 Threshold Determination

The selection of an appropriate threshold for sEMG signal segmentation is a delicate process that significantly influences the quality of the resulting signal analysis. Generally, there are two prevalent techniques for threshold determination. The first, which is utilized in this study, involves setting the threshold based on the noise characteristics within the signal, allowing for a dynamic adaptation to the signal's inherent variability [40].

The second, a more rudimentary technique, calculates the average value of the entire signal rather than isolating the noise component. This average, or percentage of it, is then used as a static threshold for segmenting the signal. While this method may be straightforward, its reliability is contingent upon the uniformity of the muscle contractions being analyzed.

It is most effective when the contractions are similar in nature and exhibit minimal variation in amplitude [22]. This method is particularly advantageous when the objective is to identify periods of peak sEMG activity, albeit at the risk of neglecting the subtler aspects of the signal's initiation and termination phases. The efficacy of the segmentation process is thus closely tied to the chosen thresholding technique. A nuanced approach, such as the one adopted in this study, can discern the intricate details of muscle activation patterns, which is essential for a comprehensive analysis of sEMG signals [40].

Conversely, the average-based method might suffice in scenarios where the detection of high-activity periods is the sole concern, despite its limitations in capturing the full spectrum of muscle activity [22].

5.4 Used Methods

The analysis of sEMG signals in this study necessitated a preprocessing step that could provide both temporal and frequency resolution with sufficient precision. For this purpose, the Short-Time Fourier Transform (STFT) was employed. The STFT was chosen for its ability to offer a detailed time-frequency distribution, which is essential for the accurate extraction of signal characteristics and subsequent segmentation [35].

While the Wavelet Transform (WT) was considered as a potential alternative due to its computational efficiency and ability to provide a similar frequency distribution, it was not utilized. The primary focus of this research was not on computational speed but rather on the segmentation efficiency and precision of temporal and frequency definition, which the STFT adequately provided [32].

Figure 5 presents the results of segmentation using other methods that were explored but ultimately not selected for the final analysis. These methods, which include Moving Average, Mean Frequency, Skewness, and Kurtosis, are depicted in the figure through four separate graphs, each illustrating the limitations that led to their exclusion.

The shortcomings of these methods rendered them unsuitable for the objectives of this study. The chosen segmentation approach required a method that could accurately delineate muscle activity while being robust against the inherent noise and variability of sEMG signals.

Consequently, despite the computational allure of the aforementioned methods, they were not adopted in favor of the STFT, which provided the necessary resolution for effective segmentation.

6 Conclusion

The comparative analysis of EMG signal segmentation methods in this study revealed the Entropy method as the most efficient for both sets of exercises. With an efficiency rate of 0.88 for the first set and 0.7592 for the second, Entropy consistently provided the highest rate of valid segment detection. This underscores its potential utility in biomechanical signal analysis, particularly in exercises varying in type and intensity.

While the RMS and Mean methods displayed commendable efficiency, the Mean method's performance notably declined in the second set of exercises. The Integral method maintained moderate efficiency across both sets, but its performance was not as consistent as that of the Entropy method. The Variance method, on the other hand, showed a significant drop in efficiency in the second set, indicating its potential limitations in diverse exercise scenarios.

These results highlight the critical role of method selection in EMG signal analysis. The Entropy method's robustness across different exercise modalities suggests its suitability for accurate and reliable EMG signal segmentation, which is crucial for biomechanical assessments and rehabilitation protocols. The study thus contributes valuable insights into the optimization of EMG analysis, enhancing the precision of biomechanical evaluations.

7 Ethical Statement

This study was performed in accordance with the Nurenberg Code. This human study was approved by Ethics Committee from Universidad Autonoma de San Luis Potosí - approval: CEI-2020-001. All adult participants provided written informed consent to participate in this study.

References

1. **Al-Ayyad, M., Owida, H. A., De-Fazio, R., Al-Naami, B., Visconti, P. (2023).** Electromyography monitoring systems in rehabilitation: A review of clinical applications, wearable devices and signal acquisition methodologies. Electronics, Vol. 12, No. 7, pp. 1520. DOI: 10.3390/electronics12071520.
2. **Anderson, A. F., Smith, M. (2009).** Progress in cartilage restoration. The American Journal of Sports Medicine, Vol. 37, No. 1, pp. 7–9. DOI: 10.1177/0363546509354205.
3. **Barbero, M., Merletti, R., Rainoldi, A. (2012).** Atlas of muscle innervation zones. Springer. DOI: 10.1007/978-88-470-2463-2.
4. **Bosnakovski, D., Chan, S. S. K., Recht, O. O., Hartweck, L. M., Gustafson, C. J., Athman, L. L., Lowe, D. A., Kyba, M. (2017).** Muscle pathology from stochastic low level DUX4 expression in an FSHD mouse model. Nature Communications, Vol. 8, No. 1, pp. 550. DOI: 10.1038/s41467-017-00730-1.
5. **Caron, R., Sinha, D., Dey, D., Polpo, A. (2018).** Categorical data analysis using a skewed weibull regression model. Entropy, Vol. 20, No. 3, pp. 176. DOI: 10.3390/e20030176.
6. **Cene, V. H., Balbinot, A. (2019).** Enhancing the classification of hand movements through sEMG signal and non-iterative methods. Health and Technology, Vol. 9, No. 4, pp. 561–577. DOI: 10.1007/s12553-019-00315-6.
7. **Chien, S. Y., Huang, Y. W., Hsieh, B. Y., Ma, S. Y., Chen, L. G. (2004).** Fast video segmentation algorithm with shadow cancellation, global motion compensation, and adaptive threshold techniques. IEEE Transactions on Multimedia, Vol. 6, No. 5, pp. 732–748. DOI: 10.1109/tmm.2004.834868.
8. **Chowdhury, R., Reaz, M., Ali, M., Bakar, A., Chellappan, K., Chang, T. (2013).** Surface electromyography signal

processing and classification techniques. Sensors, Vol. 13, No. 9, pp. 12431–12466. DOI: 10.3390/s130912431.

9. **Cram, J. R. (2012).** Introduction to Surface Electromyography. Jones and Bartlett Publishers.
10. **Dantas, J. L., Camata, T. V., Brunetto, M. A. O. C., Moraes, A. C., Abrao, T., Altimari, L. R. (2010).** Fourier and wavelet spectral analysis of EMG signals in isometric and dynamic maximal effort exercise. Proceedings of the Annual International Conference of the IEEE Engineering in Medicine and Biology, pp. 5979–5982. DOI: 10.1109/IEMBS.2010.5627579.
11. **Duan, F., Ren, X., Yang, Y. (2018).** A gesture recognition system based on time domain features and linear discriminant analysis. IEEE Transactions on Cognitive and Developmental Systems, pp. 200–208. DOI: 10.1109/TCDS.2018.2884942.
12. **Farina, D., Merletti, R., Enoka, R. M. (2004).** The extraction of neural strategies from the surface EMG. Journal of Applied Physiology, Vol. 96, No. 4, pp. 1486–1495. DOI: 10.1152/japplphysiol.01070.2003.
13. **Gao, F., Tian, T., Yao, T., Zhang, Q. (2021).** Human gait recognition based on multiple feature combination and parameter optimization algorithms. Computational Intelligence and Neuroscience, Vol. 2021, No. 1, pp. 1–14. DOI: 10.1155/2021/6693206.
14. **Hudgins, B., Parker, P., Scott, R. N. (1993).** A new strategy for multifunction myoelectric control. IEEE Transactions on Biomedical Engineering, Vol. 40, No. 1, pp. 82–94. DOI: 10.1109/10.204774.
15. **Hussain, M. S., Reaz, M. B. I., Mohd-Yasin, F., Ibrahimy, M. I. (2009).** Electromyography signal analysis using wavelet transform and higher order statistics to determine muscle contraction. Expert Systems, Vol. 26, No. 1, pp. 35–48. DOI: 10.1111/j.1468-0394.2008.00483.x.
16. **Jamaluddin, F. N., Ahmad, S. A., Mohd-Noor, S. B., Wan-Hassan, W. Z., Shair, E. F. (2018).** Performance of different threshold estimation methods on SEMG wavelet de-noising in prolonged fatigue identification. Proceedings of the IEEE-EMBS Conference on Biomedical Engineering and Sciences, IEEE, Vol. 9, pp. 293–296. DOI: 10.1109/iecbes.2018.8626599.
17. **Khan, T. I., Moznuzzaman, M., Ide, S. (2023).** Analysis of aging effect on lower limb muscle activity using short time Fourier transform and wavelet decomposition of electromyography signal. AIP Advances, Vol. 13, No. 5, pp. 055011. DOI: 10.1063/5.0148044.
18. **Kitamura, K., Tokunaga, M., Esaki, S., Hikikoshi-Iwane, A., Yanagida, T. (2005).** Mechanism of muscle contraction based on stochastic properties of single actomyosin motors observed in vitro. Biophysics, Vol. 1, pp. 1–19. DOI: 10.2142/biophysics.1.1.
19. **Li, D., Li, X., Liang, Z., Voss, L. J., Sleigh, J. W. (2010).** Multiscale permutation entropy analysis of EEG recordings during sevoflurane anesthesia. Journal of Neural Engineering, Vol. 7, No. 4, pp. 046010. DOI: 10.1088/1741-2560/7/4/046010.
20. **Lowery, M. M., Stoykov, N. S., Taflove, A., Kuiken, T. A. (2002).** A multiple-layer finite-element model of the surface EMG signal. IEEE Transactions on Biomedical Engineering, Vol. 49, No. 5, pp. 446–454. DOI: 10.1109/10.995683.
21. **Madhavan, G. (2005).** Electromyography: Physiology, engineering, and non-invasive applications. Annals of Biomedical Engineering, Vol. 33, No. 11, pp. 1653–1677. DOI: 10.1007/s10439-005-8160-y.
22. **Mendes-Junior, J. J. A., Freitas, M. B., Campos, D. P., Farinelli, F. A., Stevan, S. L., Pichorim, S. F. (2020).** Analysis of influence of segmentation, features, and classification in sEMG processing: A case study of recognition of Brazilian sign language alphabet. Sensors, Vol. 20, No. 16, pp. 4359. DOI: 10.3390/s20164359.

23. **Merletti, R., Parker, P. (2004).** Electromyography: Physiology, engineering, and noninvasive applications. John Wiley and Sons.

24. **Merletti, R., Rainoldi, A., Farina, D. (2004).** Surface electromyography for noninvasive characterization of muscle. Exercise and Sport Sciences Reviews, Vol. 29, No. 1, pp. 20–25. DOI: 10.1097/00003677-200101000-00005.

25. **Navaneethakrishna, M., Ramakrishnan, S. (2014).** Multiscale feature based analysis of surface EMG signals under fatigue and non-fatigue conditions. Proceedings of the 36th Annual International Conference of the IEEE Engineering in Medicine and Biology Society, pp. 4627–4630. DOI: 10.1109/EMBC.2014.6944655.

26. **Nazmi, N., Abdul-Rahman, M., Yamamoto, S. I., Ahmad, S., Zamzuri, H., Mazlan, S. (2016).** A review of classification techniques of EMG signals during isotonic and isometric contractions. Sensors, Vol. 16, No. 8, pp. 1304. DOI: 10.3390/s16081304.

27. **Perotto, A. O. (2011).** Anatomical guide for the electromyographer: The limbs and trunk. Charles C Thomas Pub Ltd.

28. **Phinyomark, A., Phukpattaranont, P., Limsakul, C. (2012).** Feature reduction and selection for EMG signal classification. Expert Systems with Applications, Vol. 39, No. 8, pp. 7420–7431. DOI: 10.1016/j.eswa.2012.01.102.

29. **Reaz, M. B. I., Hussain, M. S., Mohd-Yasin, F. (2006).** Techniques of EMG signal analysis: detection, processing, classification and applications. Biological Procedures Online, Vol. 8, No. 1, pp. 11–35. DOI: 10.1251/bpo115.

30. **Shannon, C. E. (1948).** A mathematical theory of communication. The Bell System Technical Journal, Vol. 27, No. 3, pp. 379–423. DOI: 10.1002/j.1538-7305.1948.tb01338.x.

31. **Shanthi, K. J., Kumar, M. S. (2007).** Skull stripping and automatic segmentation of brain MRI using seed growth and threshold techniques. Proceedings of the International Conference on Intelligent and Advanced Systems, Vol. 84, pp. 422–426. DOI: 10.1109/icias.2007.4658421.

32. **Siddique, M. F., Ahmad, Z., Ullah, N., Kim, J. (2023).** A hybrid deep learning approach: Integrating short-time fourier transform and continuous wavelet transform for improved pipeline leak detection. Sensors, Vol. 23, No. 19, pp. 8079. DOI: 10.3390/s23198079.

33. **So, R. C. H., Ng, J. K. F., Lam, R. W. K., Lo, C. K. K., Ng, G. Y. F. (2009).** EMG wavelet analysis of quadriceps muscle during repeated knee extension movement. Medicine and Science in Sports and Exercise, Vol. 41, No. 4, pp. 788–796. DOI: 10.1249/mss.0b013e31818cb4d0.

34. **Tigrini, A., Pettinari, L. A., Verdini, F., Fioretti, S., Mengarelli, A. (2021).** Shoulder motion intention detection through myoelectric pattern recognition. IEEE Sensors Letters, Vol. 5, No. 8, pp. 1–4. DOI: 10.1109/LSENS.2021.3100607.

35. **Veer, K., Agarwal, R. (2015).** Wavelet and short-time fourier transform comparison-based analysis of myoelectric signals. Journal of Applied Statistics, Vol. 42, No. 7, pp. 1591–1601. DOI: 10.1080/02664763.2014.1001728.

36. **Xiao, F., Wang, Y., He, L., Wang, H., Li, W., Liu, Z. (2019).** Motion estimation from surface electromyogram using adaboost regression and average feature values. IEEE Access, Vol. 7, pp. 13121–13134. DOI: 10.1109/access.2019.2892780.

37. **Yavuz, M., Sene, N. (2020).** Approximate solutions of the model describing fluid flow using generalized ρ-laplace transform method and heat balance integral method. Axioms, Vol. 9, No. 4, pp. 123. DOI: 10.3390/axioms9040123.

38. **Yépez-Martínez, H., Gómez-Aguilar, J. F., Atangana, A. (2018).** First integral method for non-linear differential equations with conformable derivative. Mathematical

Modelling of Natural Phenomena, Vol. 13, No. 1, pp. 14. DOI: 10.1051/mmnp/2018012.

39. **Zardoshti-Kermani, M., Wheeler, B. C., Badie, K., Hashemi, R. M. (1995).** EMG feature evaluation for movement control of upper extremity prostheses. IEEE Transactions on Rehabilitation Engineering, Vol. 3, No. 4, pp. 324–333. DOI: 10.1109/86.481972.
40. **Zhang, C., Zhou, Z., Zhou, S. (2023).** sEMG signal denoising based on variational mode decomposition and wavelet thresholding. Proceedings of the 5th International Conference on Intelligent Control, Measurement and Signal Processing, pp. 913–916. DOI: 10.1109/ICMSP58539.2023.10171095.
41. **Zhou, Y., Chen, C., Cheng, M., Alshahrani, Y., Franovic, S., Lau, E., Xu, G., Ni, G., Cavanaugh, J. M., Muh, S., Lemos, S. (2021).** Comparison of machine learning methods in sEMG signal processing for shoulder motion recognition. Biomedical Signal Processing and Control, Vol. 68, pp. 102577. DOI: 10.1016/j.bspc.2021.102577.

Article received on 28/02/2024; accepted on 05/09/2024.
**Corresponding author is Santiago Mendez-Moreno.*